tvst

Article

Edge of Scotoma Sensitivity as a Microperimetry Clinical Trial End Point in *USH2A* Retinopathy

Jason Charng[1], Tina M. Lamey[1,2], Jennifer A. Thompson[2], Terri L. McLaren[1,2], Mary S. Attia[1], Ian L. McAllister[1], Ian J. Constable[1], David A. Mackey[1], John N. De Roach[1,2], and Fred K. Chen[1,3,4]

[1] Centre of Ophthalmology and Visual Science (incorporating Lions Eye Institute), The University of Western Australia, Western Australia, Australia
[2] Australian Inherited Retinal Disease Registry and DNA Bank, Department of Medical Technology and Physics, Sir Charles Gairdner Hospital, Nedlands, Western Australia, Australia
[3] Department of Ophthalmology, Royal Perth Hospital, Perth, Western Australia, Australia
[4] Department of Ophthalmology, Perth Children's Hospital, Perth, Western Australia, Australia

Purpose: Microperimetry is commonly used to assess retinal function. We perform cross-sectional and longitudinal analysis on microperimetry parameters in *USH2A* retinopathy and explore end points suitable for future clinical trials.

Methods: Microperimetry was performed using two grids, Grid 1 (18° diameter) and Grid 2 (6° diameter). In Grid 1, four parameters (number of nonscotomatous loci, mean sensitivity [MS], responding point sensitivity [RPS], and edge of scotoma sensitivity [ESS]) were analyzed. In Grid 2, number of nonscotomatous loci and MS were examined. Interocular symmetry was also examined. Longitudinal analysis was conducted in a subset of eyes.

Results: Microperimetry could be performed in 16 of 21 patients. In Grid 1 ($n = 15$; average age, 35.6 years), average number of nonscotomatous loci, MS, RPS, and ESS were 46.6 loci, 10.0 dB, 14.7 and 9.6 dB, respectively. In Grid 2 ($n = 13$; average age, 37.4 years), 12 eyes had measurable sensitivity across the entire grid. Average MS was 23.8 dB. Interocular analysis revealed large 95% confidence intervals for all parameters. Longitudinally, Grid 1 ($n = 12$, average follow-up 2.6 years) ESS showed the fastest rate of decline (–1.84 dB/y) compared with MS (–0.34 dB/y) and RPS (–0.90 dB/y).

Conclusions: Our data suggest that ESS may be more useful than MS and RPS in test grids that cover a large extent of the macula. We caution the use of contralateral eye as an internal control.

Translational Relevance: ESS may decrease the duration or sample size of treatment trials in *USH2A* retinopathy.

Introduction

The Usherin protein is critical in the maintenance and development of neurosensory cells in the retina and inner ear, respectively.[1,2] Mutation in the encoding gene, *USH2A* (chromosome 1q41),[3] can result in isolated retinitis pigmentosa (RP; nonsyndromic) or with associated hearing loss (syndromic).[4] *USH2A* mutation has been estimated to account for approximately 11% of RP cases[5,6] and 8% of patients with inherited retinal degeneration.[7,8] Given the relatively high prevalence of *USH2A* mutations in inherited retinal degeneration, the characterization of retinal function in *USH2A* retinopathy is paramount in understanding the disease phenotype and for validating functional end points in future clinical trials.

Microperimetry is commonly used in the clinic to measure retinal sensitivity to light stimulus in the central retina. Unlike the traditional static and

translational vision science & technology

kinetic perimetric devices, the microperimeter compensates for eye movement during the test in real-time, thus allowing spatially precise projection of test stimuli onto the retinal plane. The MAIA (*Ma*cular *I*ntegrity *A*ssessment; CenterVue, Padova, Italy) device is a commercially available confocal scanning laser ophthalmoscope-based microperimeter that has demonstrated robust reliability,[9] intersession agreement,[9] and coefficient of repeatability.[10] The MAIA has been widely used in routine clinical care[11–13] as well as in monitoring retinal function in clinical trials.[14–16] More recently, the MAIA device has been used to demonstrate spatial correlation between decreased retinal sensitivity and the doughnut region bound by the double hyperautofluorescent rings[17] and the perifoveal region of reduced deep capillary plexus vessel density on optical coherence tomography angiography[18] in *USH2A* retinopathy. Several microperimetry parameters have been used for reporting structural-functional correlation and disease progression, including mean sensitivity (MS) across all test loci of the grid,[12,18–20] pointwise sensitivity,[21] zones within the test grid,[22] and the number of scotomatous or nonscotomatous (i.e., seeing) loci within the grid.[23,24] Recently, it has been reported in patients with Stargardt disease that retinal sensitivity in loci surrounding scotoma declines faster than overall MS.[25] Given the potential importance of microperimetry as a functional end point in future *USH2A* clinical trials, there is an unmet clinical need to investigate the natural history progression of *USH2A* retinopathy in microperimetry parameters.

In this study, we explored the use of MAIA microperimetry as a trial end point in *USH2A* retinopathy by using two testing grid patterns. One grid sampled across the macula while the other densely measured the fovea and parafovea. Microperimetry parameters were investigated both cross-sectionally and longitudinally in a cohort of patients with *USH2A*.

Methods

This study was approved by the human ethics committee of the University of Western Australia (RA/4/1/7916, RA/4/1/8932, RA/4/20/5454) and the Human Research Ethics Committee, Sir Charles Gairdner Hospital (2001-053) and adhered to the tenets of the Declaration of Helsinki. Written informed consent was obtained from all participants for their data to be used for research purposes.

Patient Selection

Our databases (Western Australian Retinal Disease, WARD database and Australian Inherited Retinal Disease Registry) were interrogated for patients with syndromic and nonsyndromic rod–cone dystrophy. From each group, individuals with biallelic *USH2A* mutations were selected for examination of MAIA outcome measures. This is a prospective study in which patients were scheduled to attend regular 6-monthly review sessions but the actual intervisit interval varied owing to social and logistical challenges that commonly face these patients.

Genetic Diagnosis

Genomic DNA extracted from peripheral blood[26] was analyzed by targeted next-generation sequencing, using a retinal dystrophy NGS SmartPanel (version 4 or 7; 183 or 233 genes)[27] targeting all exons and flanking intronic regions of known retinal dystrophy genes, together with known deep intronic variants. Candidate variants were confirmed by Sanger sequencing. The phase of detected candidate variants was examined by targeted Sanger sequencing of parental DNA (preferentially), and/or other familial DNA samples, as required. For patients clinically diagnosed with USH2 where segregation was incomplete, biallelism was assumed where no other variants in *USH2*-associated genes were detected. Sequencing was performed by the Casey Eye Institute Molecular Diagnostics Laboratory (Portland, OR) or the Molecular Vision Laboratory (Hillsboro, OR). Sequences were aligned to the *USH2A* reference sequence NM_206933.2, with nucleotide 1 corresponding to the A of the start codon ATG, and described in accordance with Human Genome Variation Society recommendations version 15.11.[28] Variant pathogenicity was assessed as previously described[29] and interpreted according to the American College of Medical Genetics and Genomics/Association for Molecular Pathology joint guidelines.[30]

Microperimetry Testing Protocol

MAIA microperimetry was conducted by trained ophthalmic assistants in a completely darkened room. Patients' eyes were dilated (tropicamide 0.5% and phenylephrine 2.5%) and testing was performed after the patient was given 2 to 3 minutes to adapt to the darkened condition.

Two MAIA test grids were used in this study (Supplementary Fig. S1). Where possible, these were conducted consecutively within the same session, with a brief break (1–2 minutes) between tests. Grid 1

(Supplementary Fig. S1A) samples the central 18° diameter of the macula and is composed of a 68-loci Cartesian array at 1°, 3°, 5°, 7°, and 9° from the vertical or horizontal meridian, akin to the 10-2 pattern in Humphrey visual field. Grid 2 (Supplementary Fig. S1B) covers a smaller central zone of 6° diameter, encompassing both the fovea (<2.5° radius) and the parafovea (2.5°–4.0° radius). It consists of 37 test loci distributed in a radial pattern at 0°, 1°, 2°, and 3° from the foveal center. In both grids, Goldmann III achromatic stimuli with 200-ms stimulus duration were shown on a dim white (1.27 cd/m^2) background. The differential stimulus luminance has a dynamic range spanning from 0.08 to 317.04 cd/m^2 (36 to 0 dB). In the MAIA software, 0 dB was designated to retinal loci that could only detect stimulus at the highest luminance. In addition, a location that was not detected by the subject at the highest luminance was assigned –1 dB and this convention was kept for analysis. A 4-2 test strategy was used.

Longitudinal data were available for a subset of the cohort and were measured using the follow-up testing mode provided by the MAIA manufacturer. Infrared fundus images were acquired at the first visit and used to align and register subsequent examinations. To be eligible for longitudinal analysis, the eye must have three or more visits.

Statistical Analysis

Microperimetry data from the right eye only were used for both cross-sectional and longitudinal analyses. Data from each patient's first visit were used for a cross-sectional analysis. Longitudinal data were available in a subset of patients. Interocular analysis was conducted on both eyes at the first visit, with left eye data transformed to right eye orientation.

Raw pointwise sensitivity for each test was extracted from the database within the MAIA device. For each grid, the MS across all loci and the number of nonscotomatous (sensitivity of ≥0 dB) loci were extracted. In addition, responding point,[23] which selects loci that are nonscotomatous, were also extracted for Grid 1. Responding point sensitivity (RPS) refers to the average sensitivity across all responding points within the grid. Retinal sensitivity was also extracted around the edge of the scotoma (ES) as previously proposed.[22] More specifically, ES was defined as loci adjacent to any scotomatous (i.e., –1 dB) locus (Fig. 1). In cases where there were nonscotomatous loci across the entire grid, ES analysis was performed only in eyes with scotomatous loci within the grid. For simplicity, we defined ES sensitivity (ESS) as the average sensitivity across all ES loci. In both RPS and ES, loci demarcated at first visit

were applied to subsequent visits for each individual eye. RPS and ESS analyses were not conducted in the smaller Grid 2 as the majority of the eyes (12 out of 13 cross-sectionally; 10 out of 11 longitudinally) had measurable sensitivities across the entire grid.

Unless otherwise specified, group data are summarized by average and standard deviation (SD). For longitudinal data, linear regression was fitted to each relevant parameter across time for each patient. Average slope was then calculated to give an overall estimate of change across time. Paired *t*-tests were used to compare between MAIA parameters across same eyes.
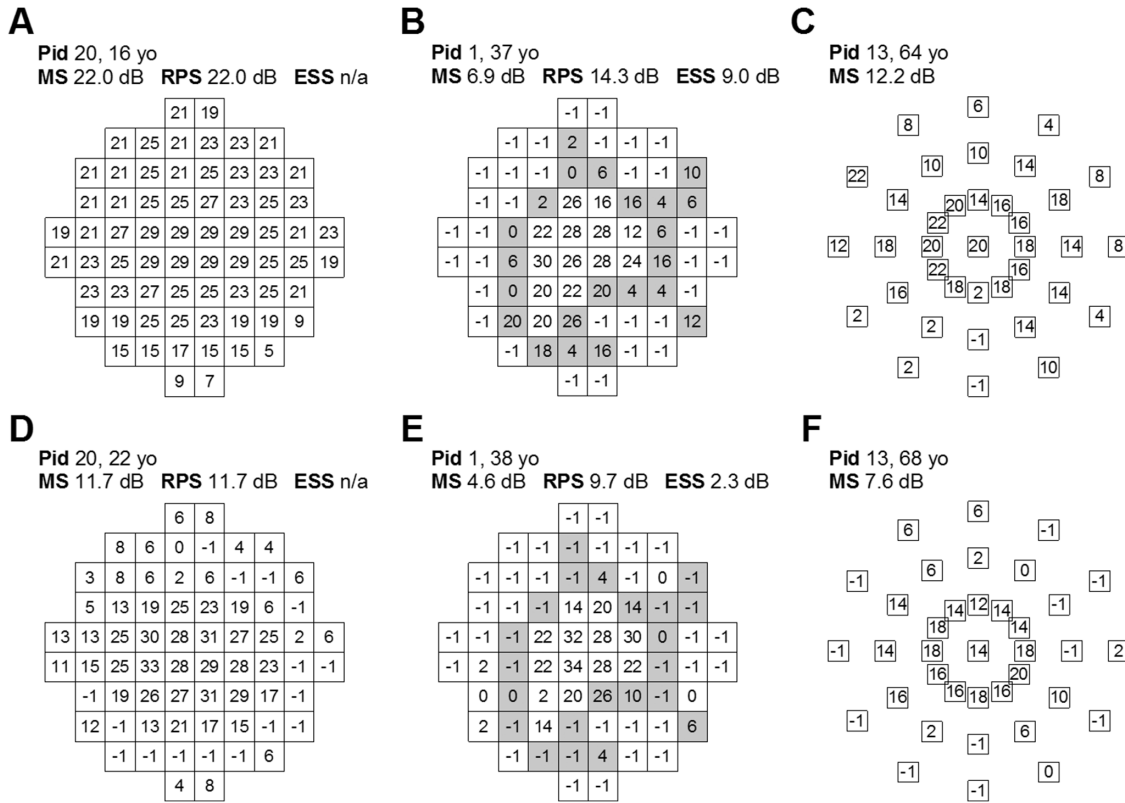
Results

Patient Demographics

A total of 175 patients with nonsyndromic RP and 27 patients with USH (10 with type 1, 17 with type 2) were identified. Of the patients with RP and USH genetically analyzed to date ($n = 106$ and $n = 27$, respectively), biallelic *USH2A* mutations were identified for six with RP (approximately 6%) and 15 with USH (approximately 56%) (Table 1). Of the 21 patients, the ratio of females to males was 3:4. The average (range) age of onset of visual symptom was 23 years (11–48 years) for the 19 patients who were symptomatic. Two asymptomatic patients were aged 4 and 7 years at their most recent follow-up.

Among the combined cohort of 21 patients with *USH2A* retinopathy, 16 were able to perform MAIA microperimetry. Of the 16 patients, 12 had testing on both grids, 3 had Grid 1 testing only and 1 had Grid 2 testing only. MAIA was not performed in five patients owing to young age ($n = 2$; patients 8 and 17), advanced disease ($n = 2$; patients 2 and 16) and patient preference ($n = 1$; patient 14). Longitudinal data were available for 12 and 11 subjects in Grids 1 and 2, respectively, with an average follow-up period of 2.9 ± 2.0 years and 2.2 ± 1.3 years for Grids 1 and 2, respectively (Supplementary Table S1).

Cross-sectional Analysis

Grid 1

For the 15 patients with MAIA data, average ± SD age was 35.6 ± 16.8 years (range, 14 –65 years). Of the 68 loci measured, the average number of nonscotomatous loci was 46.6 ± 19.4 (range, 0–68; Fig. 2A). In 11 of 15 cases, more than one-half (>34) of the test loci were detected. Linear regression estimated a

Figure 1. Extracting sensitivity parameters in Grids 1 and 2. (A, B) Grid 1 results in two different eyes at baseline. Retinal sensitivity at each locus is listed within the square. Scotoma is indicated by −1. By definition, the edge of scotoma is not applicable for (A). (B) The ES loci are marked by *grey squares*. n/a, not applicable. (C) Grid 2 results in a representative eye. Note that RPS and ESS were not extracted for this grid. (D, F) Retinal sensitivity at each eye's last visit, corresponding to the first visit plotted directly above. Note that responding points and edge of scotoma loci, defined at baseline, remain unchanged at subsequent visits.

reduction of 0.16 loci per year of age but the association was weak ($y = -0.16x + 52.5$; $R^2 = 0.02$). In addition, there seemed to be no relationship with age after stratifying the number of seeing loci into equal quarters (grey dashed lines). The average MS for the 15 eyes, across the whole of Grid 1, was 10.0 ± 6.9 dB. There was no obvious trend in MS versus age ($y = -0.11x + 13.9$; $R^2 = 0.07$; Fig. 2B). Using the conventional definition of MS (i.e., ≤24 dB regarded as below normal retinal sensitivity[10,31]; dashed line), only one eye (from the fourth oldest individual in the cohort; patient 12, age 47 years) was considered to have normal overall function. The average number of RP loci and RPS were 46.6 ± 19.4 dB and 14.6 ± 5.0 dB, respectively. Patient 18 presented with scotoma in all 68 loci so was excluded from the analysis. Note that in three eyes (patients 3, 12, and 20), there were nonscotomatous loci across the entire grid and their RPS is equivalent to their MS. The relationship between ESS and age was similar to MS and age ($y = -0.11x + 18.4$; $R^2 = 0.13$; Fig. 2C). ESS was evaluated in 11 eyes, with

patient 18 (all loci scotomatous) and patients 3, 12, and 20 (all loci nonscotomatous) not qualified for analysis. The average number of ES loci and ESS were 24.4 ± 4.4 dB and 9.6 ± 2.3 dB, respectively. There was a relatively strong association between ESS and age ($y = -0.11x + 13.2$; $R^2 = 0.49$; Fig. 2D).

Grid 2

For the 13 patients with MAIA data, the average age was 37.4 ± 16.9 years (range, 16–65 years). All 13 patients were able to detect at least 75% of the test loci in the smaller 37-loci grid (Fig. 2E). Compared with Grid 1, there was a stronger linear relationship that estimated a similar reduction of 0.07 test loci per year ($y = -0.07x + 39.0$; $R^2 = 0.23$). The average MS was 23.8 ± 6.2 dB and, in contrast with Grid 1, was accompanied with a stronger negative trend against age ($y = -0.26x + 33.4$; $R^2 = 0.49$; Fig. 2F). Correspondingly, more eyes had an MS greater than 24 dB in Grid 2 (9/13) than in Grid 1 (1/15).

Table 1. Demographic, Clinical, and Variant Data of Patients with *USH2A* Retinopathy

Patient	Sex	Syndromic	Age Onset	Age at First MAIA	RE BCVA at First MAIA	LE BCVA at First MAIA	Anterior Eye	CMO	Allele 1	Allele 2
1	Male	Yes	16	37	20/40	20/40	Mild to Moderate PSC BE	No	c.2299del	c.12697_12698del
2	Female	Yes	48	—	—	—	IOL BE	No	c.11336del	c.11336del
3	Male	No	35	62	20/25	20/20	Mild PSC BE	No	c.10073G>A	c.10073G>A
4	Female	No	15	39	20/25	20/25	Clear BE	No	c.13316C>T	c.2276G>T
5	Male	No	24	36	20/20	20/25	Clear BE	No	c.2276G>T	c.5884del
6	Male	Yes	15	32	20/40	20/40	IOL BE	BE	c.11864G>A	c.11864G>A
7	Male	Yes	16	28	20/20	20/20	Clear BE	LE only	c.10561T>C[b]	c.[3086G>T; 9258+1G>A]
8	Male	Yes	A (4)	—	—	—	Clear BE	—	c.1679del	c.2299del
9	Female	Yes	30	65	20/125	20/250	IOL BE	LE only	c.11864G>A	c.11864G>A
10	Male	Yes	11	14	20/32	20/50	Clear BE	BE	c.11864G>A[b]	c.9424G>T
11	Female	Yes	22	30	20/63	20/63	Clear BE	BE	c.7595-3C>G	c.13942_13943delinsT
12	Female	No	27	47	20/20	20/20	Clear BE	No	c.2299delG	c.2276G>T
13	Male	No	41	64	20/63	20/40	Mild NSC, PSE BE	No	c.2802T>G	c.1391G>A
14	Female	No	21	—	—	—	Clear BE	No	c.2276G>T[c]	c.5884del[c]
15	Male	Yes	18	34	20/32	20/32	PSC BE	BE	c.2299delG	c.1000C>T
16	Male	Yes	15	—	—	—	IOL BE	No	c.2299delG	exon 52 deletion
17	Female	Yes	A (7)	—	—	—	Clear BE	No	c.2299delG	exon 1-20 deletion
18	Male	Yes	44	59	20/400	20/500	IOL BE	No	c.12234_12235del	c.12234_12235del
19	Male	Yes	14	17	20/25	20/25	Clear BE	No	c.1859G>T[b]	c.12067-2A>G
20[a]	Female	Yes	15	16	20/20	20/25	Clear BE	LE only	c.949C>A	c.1256G>T
21[a]	Female	Yes	17	16	20/25	20/25	Clear BE	BE	c.949C>A	c.1256G>T

A, asymptomatic, patient's age at last examination enclosed by the bracket; BE, both eyes; CMO, cystoid macular edema; IOL, intraocular lens; PSC, posterior subcapsular cataract. USH2A reference sequence, NM_206933.2.

[a]Siblings.
[b]Biallelism assumed.
[c]Assumed variants, detected in affected sibling.
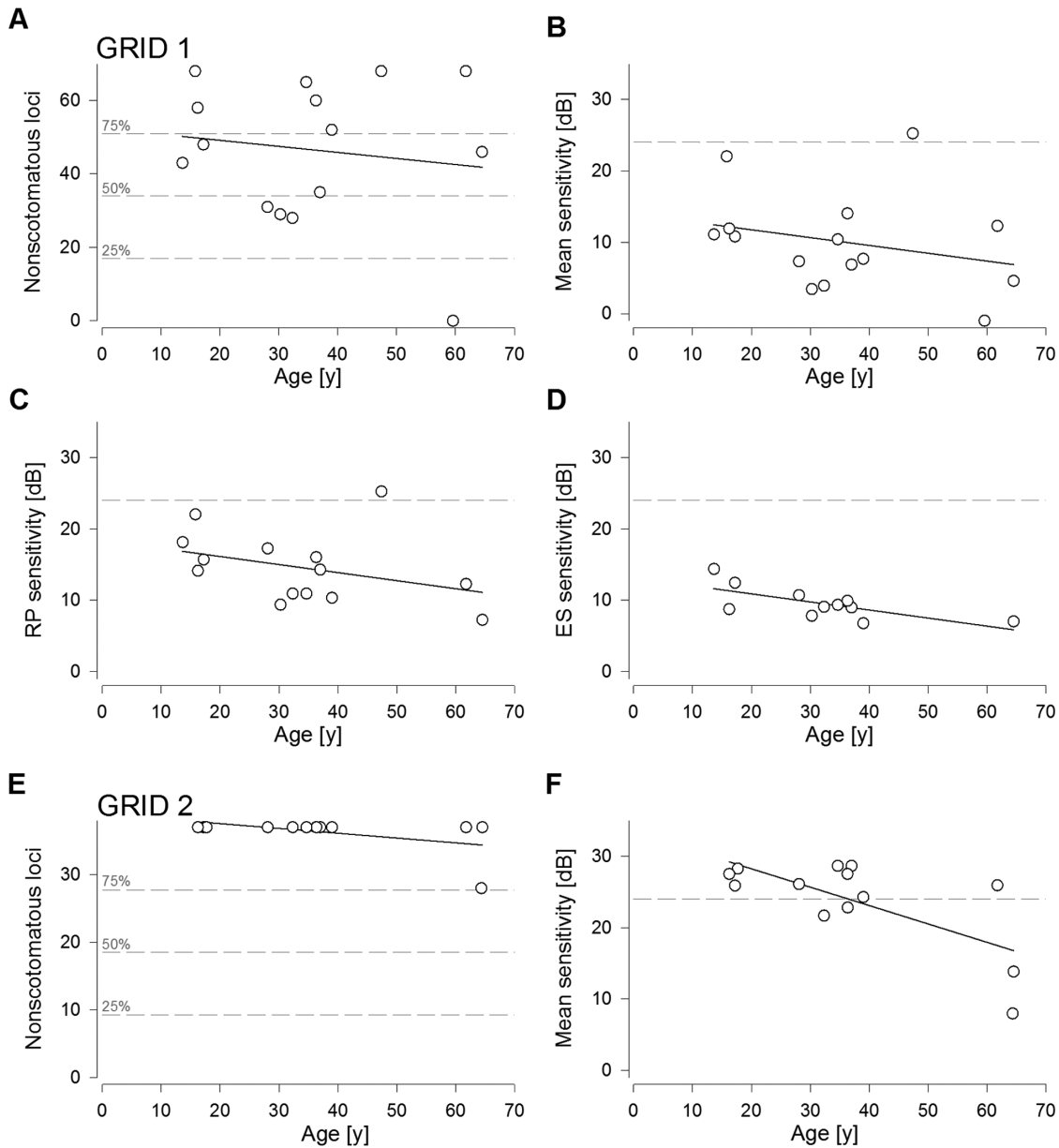
Figure 2. Cross-sectional MAIA results in *USH2A* retinopathy. (A–D) In Grid 1, the number of nonscotomatous loci (A), MS (B), RPS (C), and ESS (D) are plotted against age, respectively. Linear regression lines are plotted for each panel (*solid black*). *Grey dashed lines* in (A) divide the number of loci into quarters. *Grey dashed line* in (B, C, and D) indicates the 24 dB cut-off for normal retinal function. (E, F) In Grid 2, the number of seeing loci (E) and MS (F) are plotted against age, respectively. Other details as per (A, B).

Interocular Symmetry at Baseline

Interocular symmetry in pointwise sensitivity at the first visit was examined for Grid 1 (Fig. 3A) and Grid 2 (Fig. 3E). In both grids, symmetry was observed between contralateral eyes, as the average of the differences between right and left eyes was close to 0 (Grid 1, +0.03 dB; Grid 2, –0.06 dB). However, the 95% confidence intervals of the differences in pointwise sensitivity (dashed lines) were relatively large in both grids, with Grid 1 showing a wider interval than Grid 2

(Grid 1, –11.2 to +11.3 dB; Grid 2, –9.3 to +9.2 dB). After collapsing pointwise data into MS, the difference between the two eyes remained around 0 dB in both grids. The 95% confidence intervals of the differences in MS became tighter in both grids (Grid 1, –2.7 to +2.7 dB [Fig. 3B], Grid 2, –4.0 to +3.9 dB [Fig. 3F]). In Grid 1, the average interocular difference (95% confidence interval) in RPS (Fig. 3C) and ESS (Fig. 3D) were –0.1 dB (–3.6 to +3.5 dB) and –0.3 dB (–8.1 to +7.5).
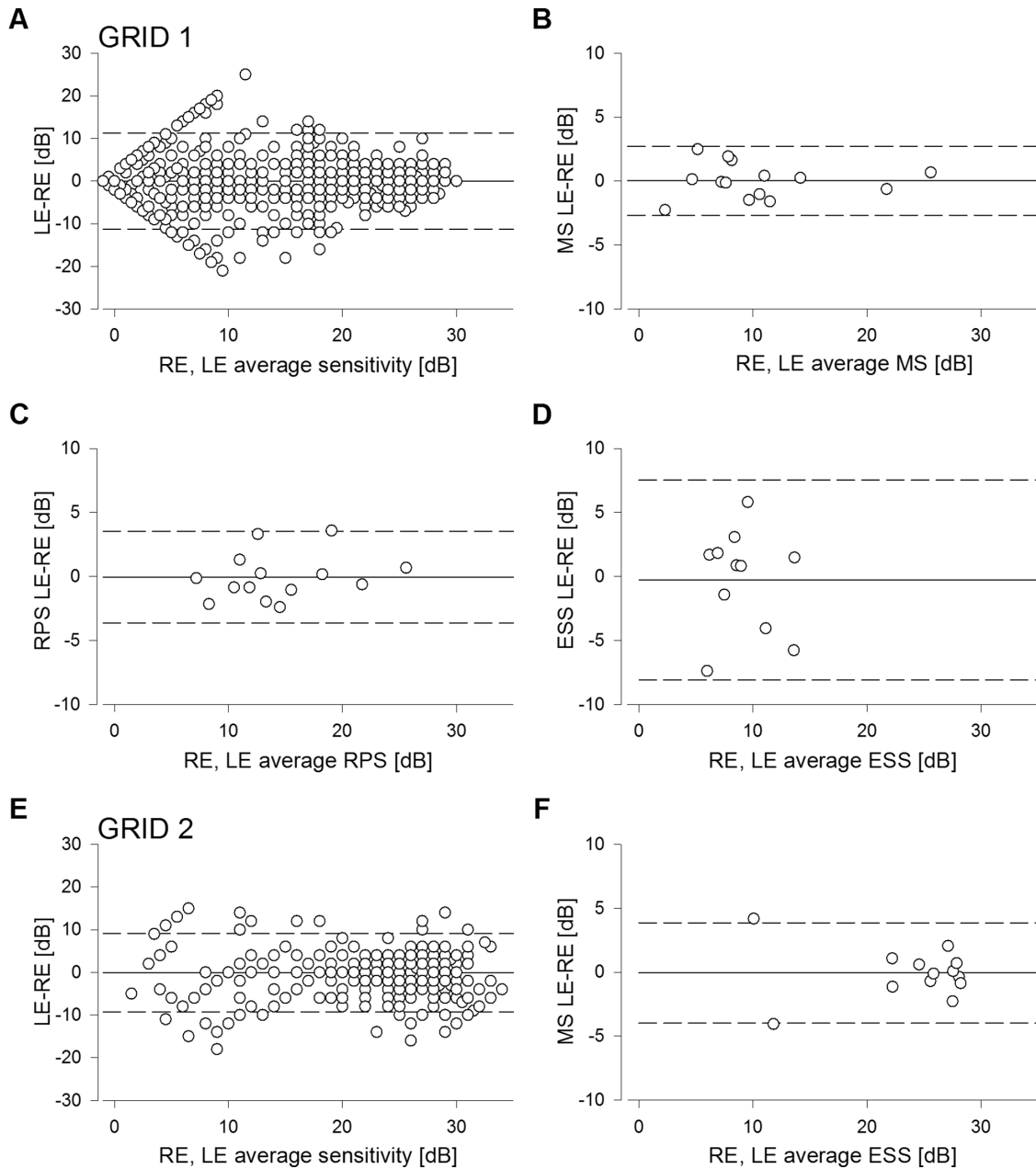
Figure 3. Cross-sectional interocular results in *USH2A* retinopathy. (A–D) In Grid 1, the differences between right and left eye in pointwise sensitivity (A), MS (B), RPS (C), and ESS (D) are plotted against their respective interocular averages. *Solid lines* indicate the average difference and the dashed lines indicate the 95% confidence interval. (E, F) In Grid 2, the differences between right and left eye in pointwise sensitivity (A) and MS (B) are plotted against their respective interocular averages. Other details as per (A).

Longitudinal Analysis

Grid 1

In the 12 patients with longitudinal data, the average follow-up period was 2.6 ± 1.7 years. The average change in the number of test loci responded was –1.4 ± 5.7 per year (Fig. 4A). Three of 12 eyes showed a paradoxical increase in the number of nonscotomatous loci across time. At the first visit, MS, RPS, and ESS showed a wide range from 3.4 to 25.3 dB, 7.3 to 25.3, and 6.8 to 14.4 dB, respectively. Note that to increase sample size, patient 20 was included in longitudinal analysis by shifting the baseline to the time when scotoma first appeared. Patient 3 and patient 12 were not included in ESS longitudinal analysis because patient 3 only had two time points with scotoma across the grid and patient 12 had nonscotomatous loci across the entire grid in all visits. The overall average MS slope indicated a decline of 0.34 ± 1.11 dB/y (Fig. 4B, Table 2). Compared with MS, RPS showed a greater
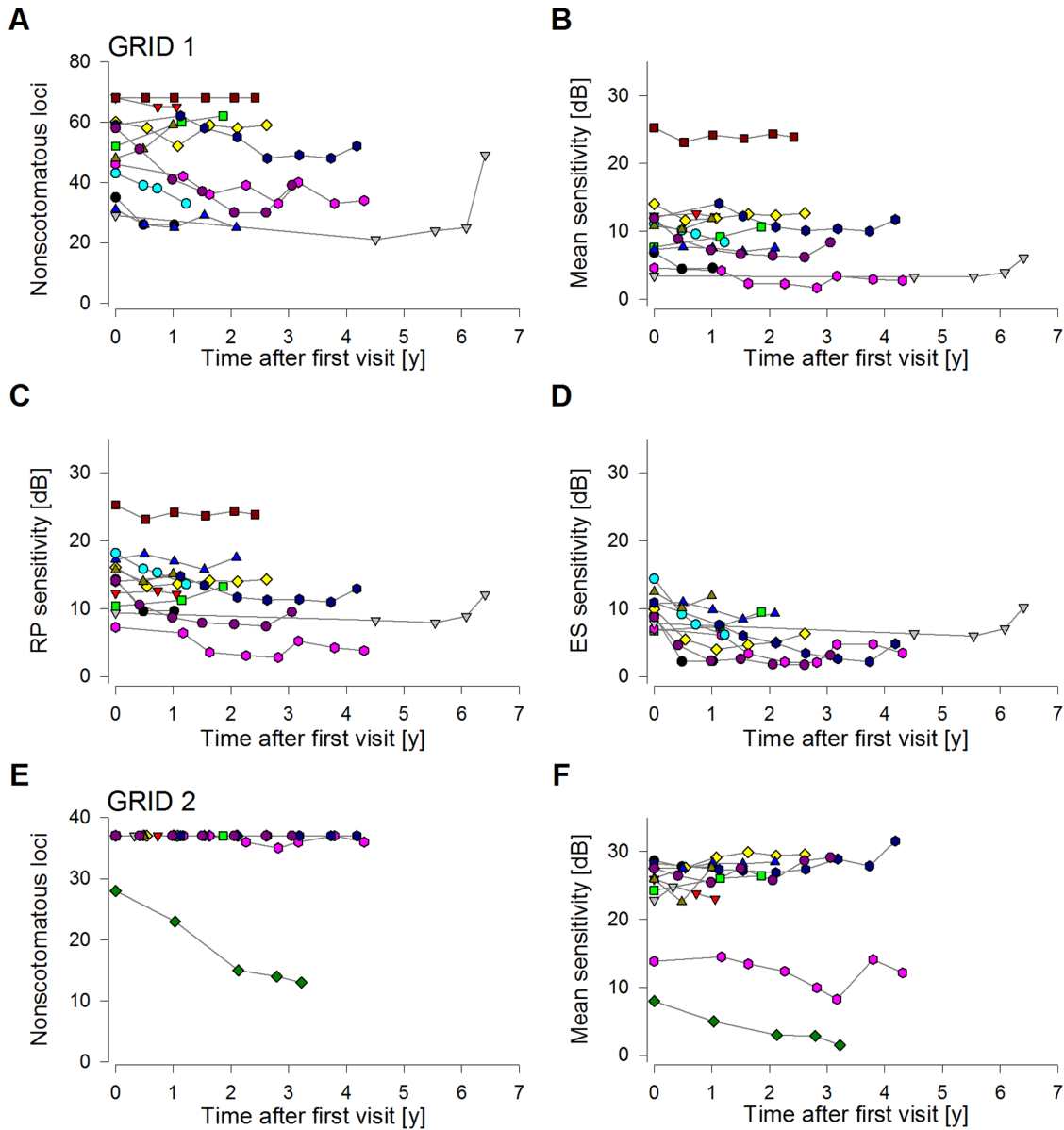
Figure 4. Longitudinal MAIA results in *USH2A* retinopathy. (A–D) In Grid 1, number of nonscotomatous loci (A), MS (B), RPS (C), and ESS (D) are plotted against time after first visit. (E, F) In Grid 2, the number of nonscotomatous loci (E) and MS (F) are plotted against time after first visit. Note that the same symbol is used for the same eye for all six panels.

average overall rate of decline at 0.90 ± 1.63 dB/y (paired *t*-test, $P < 0.05$; Fig. 4C, Table 2).Importantly, ESS showed a significantly greater decline than RPS at 1.84 (2.66) dB/y (paired *t*-test, $P < 0.05$; Fig. 4D, Table 2).

Grid 2

In the 11 patients with longitudinal data, the average follow-up period was 2.2 ± 1.3 years. Only one eye showed a decrease in the number of seeing loci across time. The remaining eyes retained stimulus detection at all 37 loci in all follow-up visits. The average change in the number of seeing loci was -0.47 ± 1.47 loci per year

(Fig. 4E). MS was greater than 20 dB at the first visit in the majority of patients (9 out of 11), and the average slope was $+0.57 \pm 2.32$ dB/y (Fig. 4F, Table 3).

Interocular Symmetry in Natural History

In Grid 1, the average difference in MS progression between right and left eyes (Fig. 5A) was 0.02 dB/y (95% confidence interval, –1.8 to +1.9 dB/y, dashed lines). The interocular difference in RPS progression was similar to MS (0.2 dB/y; Fig. 5B) but the 95% confidence interval was greater (–2.6 to 2.9 dB/y). Similarly, ESS interocular progression rates were similar between

Table 2. Linear Fit Parameters of MS, RPS, and ESS across Time in Grid 1

Patients	Longitudinal Data Points	MS		RPS		ESS	
		Slope	R^2	Slope	R^2	Slope	R^2
1	3	−2.17	0.67	−4.47	0.72	−6.50	0.72
3	3	−0.04	0.01	−0.04	0.01	—	—
4	3	+1.59	0.98	+1.49	0.88	+1.38	0.81
5	6	−0.22	0.07	−0.35	0.12	−1.05	0.23
7	5	−0.03	0.01	−0.32	0.09	−1.02	0.66
9	8	−0.38	0.30	−0.70	0.38	−0.66	0.28
10	4	−2.19	1.00	−3.65	0.98	−6.70	0.91
11	5	+0.21	0.21	+0.10	0.03	+0.05	0.01
12	6	−0.23	0.09	−0.23	0.09	—	—
19	3	+1.06	0.45	−0.55	0.10	−0.54	0.05
20	8	−0.56	0.32	−0.69	0.45	−1.77	0.74
21	7	−1.14	0.41	−1.43	0.47	−1.57	0.50
Average	5.1	−0.34	0.38	−0.90	0.36	−1.84	0.49

Table 3. Linear Fit Parameters of MS across Time in Grid 2

Patient	Longitudinal Data Points	MS	
		Slope	R^2
1	3	−0.89	0.77
3	3	−2.74	1.00
4	3	+1.20	0.95
5	6	+0.90	0.74
7	5	+1.03	0.76
9	8	−0.64	0.17
11	2	+6.13	1.00
13	5	−1.86	0.95
19	3	+1.84	0.13
20	8	+0.58	0.29
21	7	+0.66	0.29
Avg	4.8	+0.57	0.64

the two eyes (0.2 dB/y; Fig. 5C) but with wide confidence intervals (–3.3 to 3.7 dB/y). In Grid 2, the MS progression rates was similar between the two eyes (0.2 dB/y, Fig. 5D), also with relatively wide confidence interval (–2.7 to +3.0 dB/y).

Discussion

We demonstrated that MAIA was feasible in most patients with *USH2A* retinopathy. The number of test loci the patient responded to was dependent on the coverage of the testing grid used. The MS was preserved in the smaller Grid 2, but reduced in Grid 1

owing to retinal degeneration encroaching into the outer portion of this larger grid. There was good symmetry in MAIA microperimetry in both point-wise and MS , but the 95% confidence intervals were wide. In addition, we analyzed RPS and ESS in the larger Grid 1 and found that ESS rate of decline was significantly greater than that of RPS and MS, which has implication for microperimetry outcome measures in future *USH2A* clinical trials. MAIA microperimetry demonstrated highly variable longitudinal trends in the number of loci responded, MS, RPS, and ESS in *USH2A* retinopathy.

In our clinical cohort, *USH2A* retinopathy was confirmed in 6% of genetically tested patients with nonsyndromic RP and in 56% (88%) of patients with USH (USH2). In UK- and US-based studies, it has been estimated that 42% to 63% of patients with USH2[32,33] and 5% to 21% of patients with isolated RP[6,33–35] carry mutations in *USH2A*. The percentage of *USH2A* disease in our USH2 cohort is higher than previously reported but agrees with previous reports in the nonsyndromic RP cohort. This is, most likely, owing to the bias in testing specific forms of inherited retinal disease cohort related to funding availability for specific genetic research projects. Encouragingly, out of the 21 patients with confirmed biallelic *USH2A* mutations, microperimetry was feasible in the majority (16/21 [76%]), which supports its usefulness as a potential outcome measure in clinical trials.

USH2A retinopathy is a degenerative disease that progresses centripetally[36] and one would have expected that older patients may have an increased number of scotoma encroaching into the macula. However, our cross-sectional data showed a weak relationship

A

B

C

D
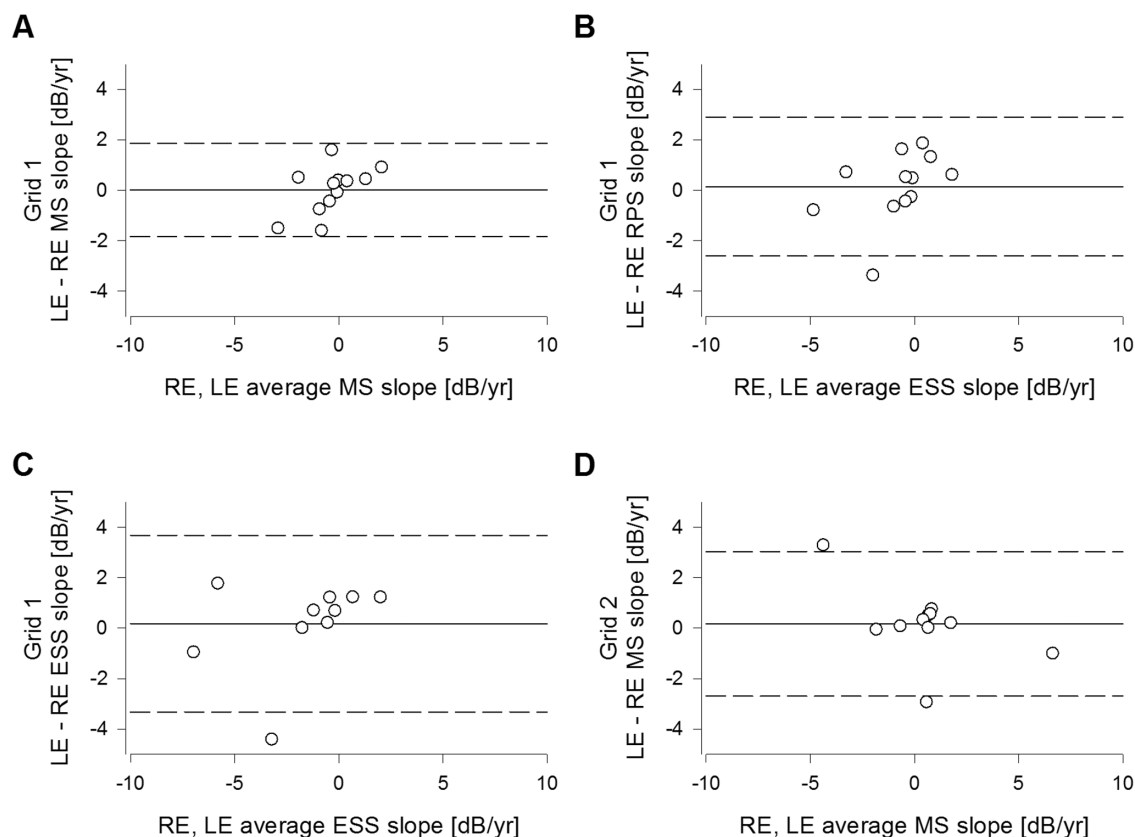
Figure 5. Longitudinal interocular results in *USH2A* retinopathy. (A–C) In Grid 1, interocular differences in MS slope (A), RPS slope (B), and ESS slope (C) are plotted against their respective interocular averages. *Solid lines* indicate the average difference and the *dashed lines* indicate the 95% confidence interval. (D) Interocular difference in MS slope is plotted against the average of both eyes in Grid 2. Other details as per (A).

between the number of nonscotomatous loci and age in the large Grid 1. In MS and RPS, there were weak negative trends with age. However, if we were to disregard the 47-year-old patient (patient 12) with an unusually high MS and RPS, the resulting R^2 values would have been much higher (MS: $y = -0.16x + 14.7$, $R^2 = 0.25$; RPS, $y = -0.17x + 19.3$, $R^2 = 0.45$). Linear fit to cross-sectional ESS data ($y = -0.11x + 13.2$, $R^2 = 0.49$) was comparable with RPS results. To our knowledge, only one study has previously examined MAIA microperimetry in *USH2A* retinopathy.[18] The authors used a grid with test loci arranged in a radial pattern covering the central 10° diameter of the macula and reported an average MS of 15.6 ± 8.2 dB in 48 eyes with biallelic variants in either *USH2A* ($n = 37$) or *MYO7A* ($n = 11$). Their average MS falls between the MS reported in the two grids in our study (Grid 1, 9.7 ± 6.9; Grid 2, 23.8 ± 6.2 dB). This finding is not surprising; the retinal coverage of the grid used in the previous study falls between the two grids used in our study (Grid 1, 20° diameter; Grid 2, 6° diameter).

Microperimetry measurements have been reported in eyes with a clinical diagnosis of RP and average MS

ranging from 5.1 to 19.3 dB.[11,37–39] However, it is difficult to directly compare these results with our study owing to the genetic heterogeneity of previous study populations and different devices and grid patterns used. Interocular symmetry is a feature in rod–cone dystrophy. Symmetry in overall macular function was supported by our observation of an almost zero difference in pointwise, mean, and ESS in both grids between the right and left eyes (Fig. 3). However, the 95% confidence intervals were relatively wide in pointwise sensitivity analysis for both grids (approximately 20 dB). In Grid 1, the 95% confidence interval was narrower in MS (5.4 dB) when compared with RPS (7.2 dB) and ESS (15.6 dB). The narrower confidence interval observed in MS may be due to the floor effect observed in the peripheral loci. In Grid 2, the 95% confidence interval of MS was also relatively large at 7.8 dB. Therefore, the wide 95% confidence intervals in the MAIA parameters should caution against the use of the fellow eye as a control in unilateral treatment trials.

In the subset of eyes with longitudinal follow-up, the average MS tended to decline in Grid 1 (–0.34 dB/y) but increase in Grid 2 (+0.57 dB/y). It is worth noting that

both trends were not statistically different from 0 dB/y, which is perhaps not surprising given the relatively short observation time in some eyes and the small sample size. In a cohort of 75 RP eyes, using the same grid pattern as Grid 1, but a different microperimetry device (Nidek MP1), it was reported that MS decreased by 0.4 dB/y,[38] which corresponds with our findings despite the genetic heterogeneity of their study cohort. To measure the change in retinal regions that are at highest risk of functional decline, we explored the use of ESS as proposed previously.[22] In Grid 1, compared with MS, the overall slope of RPS decline was approximately three-fold greater and six-fold for ESS decline. The positive average MS slope in Grid 2 (+0.57 dB/y) suggests functional preservation within the central retina in most of the cohort. Hence, the smaller retinal coverage in Grid 2 may not provide a sensitive measure of disease progression in *USH2A* until later in the disease stage when a small island of central field remains.

Our findings have implications for clinical trial design. Measuring ESS decline in a test grid with greater area of retinal coverage may enable a shorter trial period or smaller sample size compared with the use of MS or RPS. However, for grids with smaller retinal coverage, which does not cross over into regions of scotoma, RPS and ESS may not be useful outcome measures until late disease stage owing to the degeneration pattern in *USH2A*. Perhaps, instead of using a set grid, future study could investigate the usefulness of a customized grid approach.[40] However, instead of marking the central area of atrophy as suggested by the aforementioned study, which investigated patients with age-related macular degeneration, it would be more useful to mark the hyperautofluorescent ring as disease boundary in *USH2A*. Like cross-sectional data, interocular symmetry in progression rate showed an average interocular difference close to 0 dB/y in both grids for MS, RPS, and ESS. However, the 95% confidence intervals are relatively wide in all scenarios, again cautioning the use of the contralateral eyes as an internal control in a clinical trial.

Although our study examines MAIA results in patients with biallelic mutation of the *USH2A* gene, this study was based on data collected from a cohort of patients in a clinical setting. Therefore, there are several limitations to consider. First, learning effect was not examined as we had incorporated all data from all testing sessions. However, in our clinic, microperimetry is always performed in the right eye first. Hence any learning effect should be consistent across all patients. Second, test–retest variability was not addressed, which is a key factor pertinent to psychophysical tests such as microperimetry. In addition, test–retest variability is required to define significant sensitivity change across time. Future studies should determine test–retest variability of MAIA microperimetry in *USH2A* retinopathy patients across different disease severity and grids with different retinal coverage.

In conclusion, our data suggest that MAIA microperimetry may potentially serve as an outcome measure in future *USH2A* clinical trials. The technique could be performed in the majority of our cohort. Loci in the peripheral macular tend to be scotomatous or have low sensitivity values in *USH2A*, which should be considered when designing a grid pattern for testing this cohort. If indeed a test grid with wide retinal coverage is chosen in clinical trials, ESS may be a useful parameter to evaluate in this disease.

Acknowledgments

Disclosure: **J. Charng,** None; **T.M. Lamey,** None; **J.A. Thompson,** None; **T.L. Mclaren,** None; **M.S. Attia,** None; **I.L. McAllister,** None; **I.J. Constable,** None; **D.A. Mackey,** None; **J.N. De Roach,** None; **F.K. Chen,** None

References

1. Kremer H, van Wijk E, Marker T, Wolfrum U, Roepman R. Usher syndrome: molecular links of pathogenesis, proteins and pathways. *Hum Mol Genet*. 2006;15 Spec No 2:R262–R270.
2. Liu X, Bulgakov OV, Darrow KN, et al. Usherin is required for maintenance of retinal photoreceptors and normal development of cochlear hair cells. *Proc Natl Acad Sci USA*. 2007;104:4413–4418.

3. Eudy JD, Weston MD, Yao S, et al. Mutation of a gene encoding a protein with extracellular matrix motifs in Usher syndrome type IIa. *Science*. 1998;280:1753–1757.

4. Tsang SH, Aycinena ARP, Sharma T. Ciliopathy: Usher syndrome. *Adv Exp Med Biol*. 2018;1085:167–170.

5. Dockery A, Stephenson K, Keegan D, et al. Target 5000: target capture sequencing for inherited retinal degenerations. *Genes (Basel)*. 2017;8:304.

6. Ge Z, Bowles K, Goetz K, et al. NGS-based Molecular diagnosis of 105 eyeGENE((R)) probands with retinitis pigmentosa. *Sci Rep*. 2015;5:18287.

7. Carss KJ, Arno G, Erwood M, et al. Comprehensive rare variant analysis via whole-genome sequencing to determine the molecular pathology of inherited retinal disease. *Am J Hum Genet*. 2017;100:75–90.

8. Pontikos N, Arno G, Jurkute N, et al. Genetic basis of inherited retinal disease in a molecularly characterized cohort of more than 3000 families from the United Kingdom. *Ophthalmology*. 2020, Epub ahead of print.

9. Molina-Martin A, Pinero DP, Perez-Cambrodi RJ. Reliability and intersession agreement of microperimetric and fixation measurements obtained with a new microperimeter in normal eyes. *Curr Eye Res*. 2016;41:400–409.

10. Wong EN, Morgan WH, Chen FK. Intersession test-retest variability of 10-2 MAIA microperimetry in fixation-threatening glaucoma. *Clin Ophthalmol*. 2017;11:745–752.

11. Battu R, Khanna A, Hegde B, et al. Correlation of structure and function of the macula in patients with retinitis pigmentosa. *Eye (Lond)*. 2015;29:895–901.

12. Chew AL, Sampson DM, Chelva E, Khan JC, Chen FK. Perifoveal interdigitation zone loss in hydroxychloroquine toxicity leads to subclinical bull's eye lesion appearance on near-infrared reflectance imaging. *Doc Ophthalmol*. 2018;136:57–68.

13. Roh M, Lains I, Shin HJ, et al. Microperimetry in age-related macular degeneration: association with macular morphology assessed by optical coherence tomography. *Br J Ophthalmol*. 2019;103:1769–1776.

14. Chew EY, Clemons TE, Jaffe GJ, et al. Effect of ciliary neurotrophic factor on retinal neurodegeneration in patients with macular telangiectasia type 2: a randomized clinical trial. *Ophthalmology*. 2019;126:540–549.

15. Cocce KJ, Stinnett SS, Luhmann UFO, et al. Visual function metrics in early and intermediate dry age-related macular degeneration for use as clinical trial endpoints. *Am J Ophthalmol*. 2018;189:127–138.

16. Lam BL, Davis JL, Gregori NZ, et al. Choroideremia gene therapy phase 2 clinical trial: 24-month results. *Am J Ophthalmol*. 2019;197:65–73.

17. Fakin A, Sustar M, Brecelj J, et al. Double hyperautofluorescent rings in patients with USH2A-retinopathy. *Genes (Basel)*. 2019;10:956.

18. Hagag AM, Mitsios A, Gill JS, et al. Characterisation of microvascular abnormalities using OCT angiography in patients with biallelic variants in USH2A and MYO7A. *Br J Ophthalmol*. 2020;104:480–486.

19. Jones PR, Yasoubi N, Nardini M, Rubin GS. Feasibility of macular integrity assessment (MAIA) microperimetry in children: sensitivity, reliability, and fixation stability in healthy observers. *Invest Ophthalmol Vis Sci*. 2016;57:6349–6359.

20. Welker SG, Pfau M, Heinemann M, et al. Retest reliability of mesopic and dark-adapted microperimetry in patients with intermediate age-related macular degeneration and age-matched controls. *Invest Ophthalmol Vis Sci*. 2018;59:AMD152–AMD159.

21. Han RC, Jolly JK, Xue K, MacLaren RE. Effects of pupil dilation on MAIA microperimetry. *Clin Exp Ophthalmol*. 2017;45:489–495.

22. Chen FK, Patel PJ, Webster AR, et al. Nidek MP1 is able to detect subtle decline in function in inherited and age-related atrophic macular disease with stable visual acuity. *Retina*. 2011;31:371–379.

23. Meleth AD, Mettu P, Agron E, et al. Changes in retinal sensitivity in geographic atrophy progression as measured by microperimetry. *Invest Ophthalmol Vis Sci*. 2011;52:1119–1126.

24. Schonbach EM, Wolfson Y, Strauss RW, et al. Macular sensitivity measured with microperimetry in Stargardt disease in the progression of atrophy secondary to Stargardt disease (ProgStar) study: report no. 7. *JAMA Ophthalmol*. 2017;135:696–703.

25. Schonbach EM, Strauss RW, Ibrahim MA, et al. Faster sensitivity loss around dense scotomas than for overall macular sensitivity in Stargardt disease: ProgStar report no. 14. *Am J Ophthalmol*. 2020 Mar 25 [Epub ahead of print].

26. De Roach JN, McLaren TL, Paterson RL, et al. Establishment and evolution of the Australian Inherited Retinal Disease Register and DNA Bank. *Clin Exp Ophthalmol*. 2013;41:476–483.

translational vision science & technology

27. Chiang JP, Lamey T, McLaren T, et al. Progress and prospects of next-generation sequencing testing for inherited retinal dystrophy. *Expert Rev Mol Diagn*. 2015;15:1269–1275.

28. den Dunnen JT, Dalgleish R, Maglott DR, et al. HGVS recommendations for the description of sequence variants: 2016 update. *Hum Mutat*. 2016;37:564–569.

29. Thompson JA, De Roach JN, McLaren TL, et al. The genetic profile of Leber congenital amaurosis in an Australian cohort. *Mol Genet Genomic Med*. 2017;5:652–667.

30. Richards S, Aziz N, Bale S, et al. Standards and guidelines for the interpretation of sequence variants: a joint consensus recommendation of the American College of Medical Genetics and Genomics and the Association for Molecular Pathology. *Genet Med*. 2015;17:405–424.

31. Lek JJ, Brassington KH, Luu CD, et al. Subthreshold nanosecond laser intervention in intermediate age-related macular degeneration: study design and baseline characteristics of the laser in early stages of age-related macular degeneration study (report number 1). *Ophthalmol Retina*. 2017;1:227–239.

32. Leroy BP, Aragon-Martin JA, Weston MD, et al. Spectrum of mutations in USH2A in British patients with Usher syndrome type II. *Exp Eye Res*. 2001;72:503–509.

33. McGee TL, Seyedahmadi BJ, Sweeney MO, Dryja TP, Berson EL. Novel mutations in the long isoform of the USH2A gene in patients with Usher syndrome type II or non-syndromic retinitis pigmentosa. *J Med Genet*. 2010;47:499–506.

34. Lenassi E, Vincent A, Li Z, et al. A detailed clinical and molecular survey of subjects with non-syndromic USH2A retinopathy reveals an allelic hierarchy of disease-causing variants. *Eur J Hum Genet*. 2015;23:1318–1327.

35. Seyedahmadi BJ, Rivolta C, Keene JA, Berson EL, Dryja TP. Comprehensive screening of the USH2A gene in Usher syndrome type II and non-syndromic recessive retinitis pigmentosa. *Exp Eye Res*. 2004;79:167–173.

36. Pierrache LH, Hartel BP, van Wijk E, et al. Visual prognosis in USH2A-associated retinitis pigmentosa is worse for patients with Usher syndrome type IIa than for those with nonsyndromic retinitis pigmentosa. *Ophthalmology*. 2016;123:1151–1160.

37. Asahina Y, Kitano M, Hashimoto Y, et al. The structure-function relationship measured with optical coherence tomography and a microperimeter with auto-tracking: the MP-3, in patients with retinitis pigmentosa. *Sci Rep*. 2017;7:15766.

38. Iftikhar M, Kherani S, Kaur R, et al. Progression of retinitis pigmentosa as measured on microperimetry: the PREP-1 Study. *Ophthalmol Retina*. 2018;2:502–507.

39. Vingolo EM, De Rosa V, Rigoni E. Clinical correlation between retinal sensitivity and foveal thickness in retinitis pigmentosa patients. *Eur J Ophthalmol*. 2017;27:352–356.

40. Pfau M, Muller PL, von der Emde L, et al. Mesopic and dark-adapted two-color fundus-controlled perimetry in geographic atrophy secondary to age-related macular degeneration. *Retina*. 2020;40:169–180.